AIAA JOURNAL
Vol. 48, No. 8, August 2010

# Parametric Study for Dynamics of Spacecraft with Local Nonlinearities

F. Wei*
*Harbin Institute of Technology, 150001 Harbin, People's Republic of China*
and
L. Liang† and G. T. Zheng‡
*Tsinghua University, 100084 Beijing, People's Republic of China*

DOI: 10.2514/1.J050145

**Various kinds of connectors existing in most spacecraft are usually nonlinear and could strongly affect the dynamic characteristics of the spacecraft. For dynamic analysis, the spacecraft are generally idealized as finite-element models that often have huge numbers of degrees of freedom, while their connectors are spatially localized. In addition to forced harmonic response, the influences of the connectors' nonlinear parameters and/or the excitation levels on the response are also significant among major design considerations. However, it is computationally expensive to repetitively perform the analysis and computation for studying the effect of modifying nonlinear parameters and/or changing excitation levels with a direct method, especially for large-scale structures. Accordingly, an approach based on the pseudoarclength continuation scheme, the describing function, and linear receptance data is developed in the present paper. With linear receptance data, the computational efficiency of the pseudoarclength continuation scheme can be significantly enhanced and only associated with nonlinear degrees of freedom that usually constitute a small part of large-scale structures with local nonlinearities. A finite-element model of a satellite with nonlinear connectors is used to study the relationship among the response of the satellite's payloads, the excitation level, and the connectors' physical parameters.**

## Nomenclature

| | | |
|---|---|---|
| $A$ | = | amplitude of forced acceleration |
| $\mathbf{C}$ | = | damping matrix |
| $\mathbf{F}$ | = | complex amplitude of internal nonlinear forces |
| $\mathbf{f}$ | = | internal nonlinear forces |
| $f$ | = | $f$ set of external force degrees of freedom |
| $\bar{f}$ | = | number of degrees of freedom on which external forces act |
| $G$ | = | structural damping coefficient |
| $g$ | = | acceleration of gravity |
| $\mathbf{H}$ | = | receptance matrix of the derived system of a nonlinear structure |
| $\mathbf{I}$ | = | identity matrix |
| $i$ | = | $i$ set of interested degrees of freedom (excluding all nonlinear DOFs) |
| $\bar{i}$ | = | number of degrees of freedom of interest |
| $j$ | = | $\sqrt{-1}$ |
| $\mathbf{K}$ | = | stiffness matrix |
| $\mathbf{M}$ | = | mass matrix |
| $M$ | = | number of linear modes employed |
| $N$ | = | number of degrees of freedom of a structure |
| $n$ | = | $n$ set of degrees of freedom associated with nonlinear elements |
| $\bar{n}$ | = | number of degrees of freedom associated with nonlinear elements |
| $\mathbf{P}$ | = | external forces |
| $\bar{\mathbf{P}}$ | = | complex amplitude of external forces |
| $\mathbf{X}$ | = | complex amplitude of displacement |
| $\mathbf{x}, \dot{\mathbf{x}}, \ddot{\mathbf{x}}$ | = | displacement, velocity, and acceleration |
| $\omega$ | = | excitation frequency |
| $\boldsymbol{\phi}$ | = | real modes of the derived system of a nonlinear structure |
| $\boldsymbol{\psi}$ | = | complex modes of the derived system of a nonlinear structure |
| $\|\bullet\|$ | = | norm of $\bullet$ |

Received 19 August 2009; revision received 21 April 2010; accepted for publication 23 April 2010. Copyright © 2010 by the American Institute of Aeronautics and Astronautics, Inc. All rights reserved. Copies of this paper may be made for personal or internal use, on condition that the copier pay the $10.00 per-copy fee to the Copyright Clearance Center, Inc., 222 Rosewood Drive, Danvers, MA 01923; include the code 0001-1452/10 and $10.00 in correspondence with the CCC.

*Ph.D. Candidate, Department of Space Engineering and Applied Mechanics, Post Office Box 137; weifei1983@gmail.com.
†Postdoctoral Research Fellow, School of Aerospace, Post Office Box 20; llu20081025@163.com.
‡Professor, School of Aerospace, Post Office Box 20; gtzhengtu@yahoo.co.uk.

## I. Introduction

EXISTING studies [1–5] have shown that the dynamic characteristics of jointed structures could be strongly affected by nonlinear elements. In most spacecraft, there are various kinds of connectors that are usually nonlinear. Similarly, the presence of these connectors could also have obvious influences on the dynamics of spacecraft. Studies reported in [1–5] mainly focused on some simple structures to explore the nonlinear dynamic behaviors of jointed structures. Nevertheless, structures of most spacecraft are complicated, large scale, and usually idealized as finite-element (FE) models with a large number of degrees of freedom (DOFs) in engineering practices.

Direct time integration methods, such as the Newmark's method, are most commonly used to find the dynamic response of nonlinear structures. However, they are generally time consuming, and thus generally impractical for large-scale structures. Moreover, they are not often appropriate for parameter studies or designs in practical applications. Instead, forced harmonic response is usually preferred.

In many studies, the forced harmonic response of nonlinear structures is usually calculated with several commonly used methods, such as the harmonic balance (HB) method [6], the describing function (DF) method [7], and the alternating frequency time method [8]. Tanrikulu et al. [9] developed an effective approach based on the DF to study the harmonic vibration of multi-DOF structures with local nonlinearities. Ciğerogğlu and Özgüven [10] adopted a similar method to analyze the nonlinear vibration of bladed disks with dry friction dampers. Ferreira and Serpa [11] used the DF and the arclength method of Crisfield [12] to study several simple nonlinear spring-mass systems. Difficulties can arise when these frequency

domain methods are directly used for large-scale structures. Before using them, many scholars reduced the size of the problem by taking advantage of several model reduction methods [13–17]. To avoid the problem of accuracy deterioration caused by the model reduction, the authors of [18] applied the DF and linear receptance data to calculate the forced harmonic response of structures with local nonlinearities. The computational effort was significantly reduced, as the calculation is only related with nonlinear DOFs.

The pseudoarclength continuation scheme is a well-known numerical path following method to solve parametric nonlinear equations. It has been applied to analyze the dynamic response of nonlinear structures in many studies. Sundararajan and Noah [19] combined the shooting method with the pseudoarclength scheme to study a rigid rotor supported on symmetrical squeeze-film dampers and journal bearings. In [20], a fixed-interface component mode synthesis method was first applied to obtain a reduced model of a large-order system with local nonlinearities. Then, the model was studied with the method presented in [19]. Padmanabhan and Singh [21] adopted a path following scheme with the shooting method to discuss the time domain response of piecewise nonlinear structures under periodical excitation. Von Groll and Ewins [22] applied the HB method with the pseudoarclength method to investigate the nonlinear dynamic response of a Jeffcott rotor with stator. In [23], the influences of impact damping on the frequency domain response of a torsional system with clearance were studied by the approach described in [22]. A similar approach was also chosen to study the geometrically nonlinear vibration of thick plates [24] and shells [25].

Except for forced harmonic response itself, the effects of modifications to nonlinear parameters and/or variations in excitation levels on the forced harmonic response are also of great importance to structural designs. Repetitively calculating the response during the variation of nonlinear parameters and/or excitation levels is often taken as a direct approach for this purpose. Obviously, this procedure will be computationally expensive, especially for large-scale structures. Thus, an efficient and convenient computation method is expected. To solve the preceding problem, a new method will be developed in the present paper.

The method developed in [18] is first applied to obtain the equations of motion in frequency domain. Subsequently, the pseudoarclength scheme is used to solve the nonlinear equations. If the scalar parameter is chosen to be the frequency of excitation, this scheme can be applied to compute the forced harmonic response of structures with local nonlinearities. In the solution of forced harmonic response, the pseudoarclength continuation scheme can provide a complete description of forced harmonic response curves, and it is more robust than other simple iterative procedures, such as the Newton–Raphson method and the iterative schemes used in [9,10,18]. For overcoming the problem of highly expensive computation costs, linear receptance data are used to reduce the number of DOFs involved in the computation to the number of nonlinear DOFs, which usually constitute only a small part of a large-scale structure with local nonlinearities.

## II. Mathematical Formulation

In this section, the concept of the method proposed in [18] is briefly reviewed for the subsequent study. Viscous damping matrix is included in the dynamic equations of motion of a structure with local nonlinearities, used in [18], to generalize the equations; thus, there is a set of ordinary differential equations,

$$\mathbf{M}\ddot{\mathbf{x}} + \mathbf{C}\dot{\mathbf{x}} + (1 + jG)\mathbf{K}\mathbf{x} + \mathbf{f}(\mathbf{x}, \dot{\mathbf{x}}) = \mathbf{P}(t) \tag{1}$$

where the harmonic excitation of the structure is given as

$$\mathbf{P} = \bar{\mathbf{P}}e^{j\omega t} \tag{2}$$

If the nonlinearities considered are symmetric or weak, the subharmonic response can be generally ignored when compared with the fundamental response [21]. Hence, the response can be approximated by

$$\mathbf{x} = \mathbf{X}e^{j\omega t} \tag{3}$$

As the response is harmonic, the internal nonlinear forces can also be taken as harmonic, which are

$$\mathbf{f} = \mathbf{F}e^{j\omega t} \tag{4}$$

Substituting Eqs. (2–4) into Eq. (1) and using linear receptance data yields

$$\mathbf{X}_n = \mathbf{N}_n - \mathbf{H}_{nn}\mathbf{F}_n \tag{5}$$

$$\mathbf{X}_i = \mathbf{N}_i - \mathbf{H}_{in}\mathbf{F}_n \tag{6}$$

where

$$\mathbf{H} = (-\omega^2\mathbf{M} + j\omega\mathbf{C} + (1 + jG)\mathbf{K})^{-1}$$

$\mathbf{N}_n = \mathbf{H}_{nf}\bar{\mathbf{P}}_f$, and $\mathbf{N}_i = \mathbf{H}_{if}\bar{\mathbf{P}}_f$.

Splitting Eqs. (5) and (6) into real and imaginary parts leads to

$$\begin{Bmatrix} \mathrm{Re}(\mathbf{X}_n) \\ \mathrm{Im}(\mathbf{X}_n) \end{Bmatrix} = \begin{Bmatrix} \mathrm{Re}(\mathbf{N}_n) \\ \mathrm{Im}(\mathbf{N}_n) \end{Bmatrix} - \begin{bmatrix} \mathrm{Re}(\mathbf{H}_{nn}) & -\mathrm{Im}(\mathbf{H}_{nn}) \\ \mathrm{Im}(\mathbf{H}_{nn}) & \mathrm{Re}(\mathbf{H}_{nn}) \end{bmatrix} \begin{Bmatrix} \mathrm{Re}(\mathbf{F}_n) \\ \mathrm{Im}(\mathbf{F}_n) \end{Bmatrix} \tag{7}$$

$$\begin{Bmatrix} \mathrm{Re}(\mathbf{X}_i) \\ \mathrm{Im}(\mathbf{X}_i) \end{Bmatrix} = \begin{Bmatrix} \mathrm{Re}(\mathbf{N}_i) \\ \mathrm{Im}(\mathbf{N}_i) \end{Bmatrix} - \begin{bmatrix} \mathrm{Re}(\mathbf{H}_{in}) & -\mathrm{Im}(\mathbf{H}_{in}) \\ \mathrm{Im}(\mathbf{H}_{in}) & \mathrm{Re}(\mathbf{H}_{in}) \end{bmatrix} \begin{Bmatrix} \mathrm{Re}(\mathbf{F}_n) \\ \mathrm{Im}(\mathbf{F}_n) \end{Bmatrix} \tag{8}$$

To make the following discussions clear, Eqs. (7) and (8) and are rewritten in a compact form:

$$\bar{\mathbf{X}}_n = \bar{\mathbf{N}}_n - \bar{\mathbf{H}}_{nn}\bar{\mathbf{F}}_n \tag{9}$$

$$\bar{\mathbf{X}}_i = \bar{\mathbf{N}}_i - \bar{\mathbf{H}}_{in}\bar{\mathbf{F}}_n \tag{10}$$

where the nonlinear term $\bar{\mathbf{F}}_n$ can be quasi linearized and expressed as

$$\bar{\mathbf{F}}_n = \begin{bmatrix} \mathrm{Re}(\boldsymbol{\Delta}) & -\mathrm{Im}(\boldsymbol{\Delta}) \\ \mathrm{Im}(\boldsymbol{\Delta}) & \mathrm{Re}(\boldsymbol{\Delta}) \end{bmatrix} \bar{\mathbf{X}}_n \tag{11}$$

In the above equation, $\boldsymbol{\Delta}$ is a generalized quasi-linear matrix for which the elements can be calculated by the DF, and it can be written as

$$\Delta_{rr} = \nu_{rr} + \sum_{s=1, s\neq r}^{n} \nu_{rs} \tag{12}$$

$$\Delta_{rs} = -\nu_{rs} \tag{13}$$

where

$$\nu_{rs} = \frac{\omega}{\pi Z} j \int_{-\pi/\omega}^{\pi/\omega} f_{rs} e^{-j\omega t}\, \mathrm{d}t; \qquad Z = \begin{cases} X_r - X_s & r \neq s \\ X_r & r = s \end{cases} \tag{14}$$

Substituting Eq. (11) into Eq. (9) and (10) yields

$$\bar{\mathbf{H}}_{nn}\bar{\boldsymbol{\Delta}}\bar{\mathbf{X}}_n + \bar{\mathbf{X}}_n - \bar{\mathbf{N}}_n = \mathbf{0} \tag{15}$$

$$\bar{\mathbf{X}}_i = \bar{\mathbf{N}}_i - \bar{\mathbf{H}}_{in}\bar{\boldsymbol{\Delta}}\bar{\mathbf{X}}_n \tag{16}$$

## III. Solution Method

In Sec. II, the set of $N$-order nonlinear ordinary differential equations has been converted to a set of $(2\bar{i} + 2\bar{n})$ algebraic equations. It is obvious that the algebraic equations should be solved iteratively. It should be mentioned that the nonlinear matrix $\bar{\boldsymbol{\Delta}}$ is only dependent on the response of nonlinear DOFs (i.e., $\bar{\mathbf{X}}_n$).

Thus, by solving Eq. (15) iteratively, the computation effort can be reduced and only related to nonlinear DOFs. After $\bar{\mathbf{X}}_n$ is obtained by the pseudoarclength continuation scheme, $\bar{\mathbf{X}}_i$ can be easily determined with Eq. (16).

Equation (15) describes a set of nonlinear algebraic equations that are a function of displacement, excitation frequency, excitation levels, and parameters of nonlinear elements. For the sake of convenience, subscript $n$ is ignored in the subsequent analysis, and the equation is rewritten as

$$\Im(\bar{\mathbf{X}}, \lambda) = \mathbf{0} \tag{17}$$

where $\lambda$ is a scalar parameter that is used to represent either the frequency of excitation or a parameter of a nonlinear element, or the excitation level.

The pseudoarclength continuation scheme will be adopted to solve Eq. (17). In the following part, the pseudoarclength continuation scheme and calculations of linear receptance data will be outlined.

### A. Pseudoarclength Continuation Scheme

Here, the pseudoarclength continuation scheme is briefly discussed. One can refer to [26,27] for more details.

Taking the differential of Eq. (17), one can have the following equation, which is often called the Davidenko differential equation:

$$\frac{\mathrm{d}\bar{\mathbf{X}}}{\mathrm{d}\lambda} = -\Im_{\bar{\mathbf{X}}}^{-1}(\bar{\mathbf{X}}, \lambda)\Im_{\lambda}(\bar{\mathbf{X}}, \lambda) \tag{18}$$

where $\Im_{\bar{\mathbf{X}}} = \frac{\partial \Im}{\partial \bar{\mathbf{X}}}$ and $\Im_{\lambda} = \frac{\partial \Im}{\partial \lambda}$.

The procedure will fail when $\Im_{\bar{\mathbf{X}}}(\bar{\mathbf{X}}, \lambda)$ is singular. To overcome this limitation, the arclength $s$ is used as a continuation parameter; thus, both $\mathbf{X}$ and $\lambda$ are functions of $s$. Then, differentiating Eq. (17) with respect to $s$ yields

$$\Im_{\bar{\mathbf{X}}}(\bar{\mathbf{X}}, \lambda)\mathbf{X}' + \Im_{\lambda}(\bar{\mathbf{X}}, \lambda)\lambda' = \{\Im_{\bar{\mathbf{X}}} | \Im_{\lambda}\}\mathbf{t} = \mathbf{0} \tag{19}$$

where $\mathbf{t} = \{\bar{\mathbf{X}}'^T, \lambda'\}^T$, $\bar{\mathbf{X}}' = \mathrm{d}\bar{\mathbf{X}}/\mathrm{d}s$, and $\lambda' = \mathrm{d}\lambda/\mathrm{d}s$. In addition, the tangent vector $\mathbf{t}$ satisfies the following normalizing condition:

$$\bar{\mathbf{X}}'^T\bar{\mathbf{X}}' + \lambda'^2 = \bar{X}_1'^2 + \bar{X}_2'^2 + \cdots + \bar{X}_n'^2 + \lambda'^2 = 1 \tag{20}$$

which implies that $\mathbf{t}$ is a vector of unit length.

The tangent vector $\mathbf{t}$ can be calculated by

$$\begin{cases} \Im_{\bar{\mathbf{X}}}(\bar{\mathbf{X}}, \lambda)\mathbf{z} = -\Im_{\lambda}(\bar{\mathbf{X}}, \lambda) \\ \lambda' = \sigma(1 + \mathbf{z}^T\mathbf{z})^{-1/2} \\ \bar{\mathbf{X}}' = \lambda'\mathbf{z} \end{cases} \tag{21}$$

where $\sigma = \pm 1$ is chosen to make the orientation of the continuation continue without changing. Assuming that $(\bar{\mathbf{X}}_{-1}'^T, \lambda_{-1}')^T$ is the preceding tangent vector, the following should be satisfied:

$$\lambda'(\bar{\mathbf{X}}_{-1}'^T\mathbf{z} + \lambda_{-1}') > 0 \tag{22}$$

The tangent predictor is usually used to predict values of $\bar{\mathbf{X}}$ and $\lambda$ at $s + \Delta s$; that is,

$$\bar{\mathbf{X}} = \bar{\mathbf{X}}_0 + \bar{\mathbf{X}}'\Delta s; \qquad \lambda = \lambda_0 + \lambda'\Delta s \tag{23}$$

If $(\bar{\mathbf{X}}^*, \lambda^*)$ is a regular point on the path and $\mathbf{t}^* = \{\bar{\mathbf{X}}^{*\prime T}, \lambda^{*\prime}\}^T$ is the unit tangent vector at this point, the parameterization equation of the pseudoarclength continuation scheme can be given by

$$\mathbf{g}(\bar{\mathbf{X}}, \lambda) = (\bar{\mathbf{X}} - \bar{\mathbf{X}}^*)^T\bar{\mathbf{X}}^{*\prime} + (\lambda - \lambda^*)\lambda^{*\prime} - \Delta s = 0 \tag{24}$$

Then Eqs. (17–24) constitute the pseudoarclength continuation scheme. The following equations can be obtained by the Newton–Raphson method:

$$\begin{cases} \Im_{\bar{\mathbf{X}}}(\bar{\mathbf{X}}^k, \lambda^k)\Delta\bar{\mathbf{X}}^k + \Im_{\lambda}(\bar{\mathbf{X}}^k, \lambda^k)\Delta\lambda^k = -\Im(\bar{\mathbf{X}}^k, \lambda^k) \\ (\bar{\mathbf{X}}^{*\prime})^T\Delta\bar{\mathbf{X}}^k + \lambda^{*\prime}\Delta\lambda^k = -\mathbf{g}(\bar{\mathbf{X}}^k, \lambda^k) \end{cases} \tag{25}$$

Using the pseudoarclength scheme, the coefficient matrix of Eq. (25) is always nonsingular. The equation can be solved by the bordering algorithm [28]. Hence, the next iteration can be evaluated by $\bar{\mathbf{X}}^{k+1} = \bar{\mathbf{X}}^k + \Delta\bar{\mathbf{X}}^k$ and $\lambda^{k+1} = \lambda^k + \Delta\lambda^k$.

### B. Calculations of Linear Receptance Data

In Sec. I, $\mathbf{H}_{nf}$, $\mathbf{H}_{if}$, $\mathbf{H}_{nn}$, and $\mathbf{H}_{in}$ can be computed by means of matrix inversion, which is generally time consuming. Alternatively, with the linear mode superposition method, the matrix inversion can be totally avoided.

If the viscous damping matrix $\mathbf{C}$ is generalized proportionally, it can be diagonalized with real modes. The relationship can be described as

$$\boldsymbol{\phi}^T\mathbf{C}\boldsymbol{\phi} = \mathrm{diag}(\,\zeta_1 \quad \zeta_2 \quad \cdots \quad \zeta_N\,) \tag{26}$$

In this case, $\mathbf{H}_{nf}$, $\mathbf{H}_{if}$, $\mathbf{H}_{nn}$, and $\mathbf{H}_{in}$ can be calculated by

$$\begin{aligned} \mathbf{H}_{nn} &= [\,\phi_{n1} \quad \cdots \quad \phi_{nM}\,]\boldsymbol{\Lambda}[\,\phi_{n1} \quad \cdots \quad \phi_{nM}\,]^T; \\ \mathbf{H}_{nf} &= [\,\phi_{n1} \quad \cdots \quad \phi_{nM}\,]\boldsymbol{\Lambda}[\,\phi_{f1} \quad \cdots \quad \phi_{fM}\,]^T; \\ \mathbf{H}_{if} &= [\,\phi_{i1} \quad \cdots \quad \phi_{iM}\,]\boldsymbol{\Lambda}[\,\phi_{f1} \quad \cdots \quad \phi_{fM}\,]^T; \\ \mathbf{H}_{in} &= [\,\phi_{i1} \quad \cdots \quad \phi_{iM}\,]\boldsymbol{\Lambda}[\,\phi_{n1} \quad \cdots \quad \phi_{nM}\,]^T \end{aligned} \tag{27}$$

where $\boldsymbol{\Lambda}$ is a diagonal matrix that can be given by

$$\boldsymbol{\Lambda} = \mathrm{diag}\left(\frac{1}{j\omega\zeta_1 + (1 + jG)\omega_1^2 - \omega^2} \quad \cdots \quad \frac{1}{j\omega\zeta_M + (1 + jG)\omega_M^2 - \omega^2}\right) \tag{28}$$

If the viscous damping matrix $\mathbf{C}$ is nonproportional, similar expressions can be obtained by using complex modes, and they can be given by

$$\begin{aligned} \mathbf{H}_{nn} &= [\,\psi_{n1} \quad \cdots \quad \psi_{nM}\,]\boldsymbol{\chi}[\,\psi_{n1} \quad \cdots \quad \psi_{nM}\,]^T \\ &\quad + [\,\psi_{n1}^* \quad \cdots \quad \psi_{nM}^*\,]\boldsymbol{\chi}^*[\,\psi_{n1}^* \quad \cdots \quad \psi_{nM}^*\,]^T; \\ \mathbf{H}_{nf} &= [\,\psi_{n1} \quad \cdots \quad \psi_{nM}\,]\boldsymbol{\chi}[\,\psi_{f1} \quad \cdots \quad \psi_{fM}\,]^T \\ &\quad + [\,\psi_{n1}^* \quad \cdots \quad \psi_{nM}^*\,]\boldsymbol{\chi}^*[\,\psi_{f1}^* \quad \cdots \quad \psi_{fM}^*\,]^T; \\ \mathbf{H}_{if} &= [\,\psi_{i1} \quad \cdots \quad \psi_{iM}\,]\boldsymbol{\chi}[\,\psi_{f1} \quad \cdots \quad \psi_{fM}\,]^T \\ &\quad + [\,\psi_{i1}^* \quad \cdots \quad \psi_{iM}^*\,]\boldsymbol{\chi}^*[\,\psi_{f1}^* \quad \cdots \quad \psi_{fM}^*\,]^T; \\ \mathbf{H}_{in} &= [\,\psi_{i1} \quad \cdots \quad \psi_{iM}\,]\boldsymbol{\chi}[\,\psi_{n1} \quad \cdots \quad \psi_{nM}\,]^T \\ &\quad + [\,\psi_{i1}^* \quad \cdots \quad \psi_{iM}^*\,]\boldsymbol{\chi}^*[\,\psi_{n1}^* \quad \cdots \quad \psi_{nM}^*\,]^T \end{aligned} \tag{29}$$

where

$$\begin{aligned} \boldsymbol{\chi} &= \mathrm{diag}\left(\frac{1}{j\omega a_1 + b_1}, \cdots, \frac{1}{j\omega a_M + b_M}\right); \\ \boldsymbol{\chi}^* &= \mathrm{diag}\left(\frac{1}{j\omega a_1^* + b_1^*}, \cdots, \frac{1}{j\omega a_M^* + b_M^*}\right) \end{aligned} \tag{30}$$

In Eq. (30), $a_1, \ldots, a_M, b_1, \ldots, b_M, a_1^*, \ldots, a_M^*$, and $b_1^*, \ldots, b_M^*$ are given by

$$\begin{aligned} &\mathrm{diag}(a_1, \ldots, a_n, a_1^*, \ldots, a_n^*) \\ &\quad = \begin{bmatrix} \boldsymbol{\psi} & \boldsymbol{\psi}^* \\ \boldsymbol{\psi}\boldsymbol{\Lambda} & \boldsymbol{\psi}^*\boldsymbol{\Lambda}^* \end{bmatrix}^T \begin{bmatrix} \mathbf{C} & \mathbf{M} \\ \mathbf{M} & \mathbf{0} \end{bmatrix} \begin{bmatrix} \boldsymbol{\psi} & \boldsymbol{\psi}^* \\ \boldsymbol{\psi}\boldsymbol{\Lambda} & \boldsymbol{\psi}^*\boldsymbol{\Lambda}^* \end{bmatrix} \end{aligned} \tag{31}$$

$$\begin{aligned} &\mathrm{diag}(b_1, \cdots, b_n, b_1^*, \cdots, b_n^*) \\ &\quad = \begin{bmatrix} \boldsymbol{\psi} & \boldsymbol{\psi}^* \\ \boldsymbol{\psi}\boldsymbol{\Lambda} & \boldsymbol{\psi}^*\boldsymbol{\Lambda}^* \end{bmatrix}^T \begin{bmatrix} (1 + jG)\mathbf{K} & \mathbf{0} \\ \mathbf{0} & -\mathbf{M} \end{bmatrix} \begin{bmatrix} \boldsymbol{\psi} & \boldsymbol{\psi}^* \\ \boldsymbol{\psi}\boldsymbol{\Lambda} & \boldsymbol{\psi}^*\boldsymbol{\Lambda}^* \end{bmatrix} \end{aligned} \tag{32}$$

where

$$\mathbf{\Lambda} = \text{diag}(-b_1/a_1, \ \ldots, -b_M/a_M);$$
$$\mathbf{\Lambda}^* = \text{diag}(-b_1^*/a_1^*, \ \ldots, -b_M^*/a_M^*) \tag{33}$$

It should be noted that the superscript $*$ in Eqs. (29–33) represents complex conjugates if $G = 0$ (i.e., only nonproportional viscous damping is considered in the structure).

The accuracy of $\mathbf{H}_{nf}$, $\mathbf{H}_{if}$, $\mathbf{H}_{nn}$, and $\mathbf{H}_{in}$ heavily depends on the number of employed linear modes, so it would need more modes to achieve a satisfactory result.

### C. Solution Procedure Description

If a local nonlinear structure is excited by a harmonic force with frequency $\omega_l$, the value of a nonlinear parameter $\lambda$ is changed from $\lambda_o$ to $\lambda_\upsilon$. It is assumed that the forced harmonic response ($\lambda = \lambda_o$) of a structure's nonlinear DOFs has been obtained or given. In the calculation, the modified nonlinear parameter $\lambda$ can be used as a scalar parameter in Eq. (17). Meanwhile, the response of the nonlinear DOFs ($\lambda = \lambda_o$) is used as the initial conditions. Then, the forced harmonic response for a modified structure ($\lambda = \lambda_o$) can be calculated with the pseudoarclength continuation method. A procedure of the approach is sketched in Fig. 1. As the arc length $s$ is used as a step-length control parameter in the pseudoarclength continuation scheme, the results obtained are usually very close to the exact solutions at $\lambda_\upsilon$. Thus, the third Lagrange interpolation polynomial is used to predict the solutions at $\lambda_\upsilon$, which can be expressed as

$$\bar{\mathbf{X}}_i(\lambda_\upsilon) = \prod_{\tau=1}^{3} l_\tau(\lambda_\upsilon)\bar{\mathbf{X}}_\tau^i \tag{34}$$

where

$$l_\tau = \prod_{\kappa=1,\kappa\neq\tau}^{3} \frac{(\lambda - \lambda_\kappa)}{(\lambda_\tau - \lambda_\kappa)}; \qquad \tau = \upsilon - 3, \ \upsilon - 2, \ \upsilon - 1; \qquad \upsilon = 4 \tag{35}$$

Furthermore, calculations for effects of nonlinear parameters and/or excitation levels in a certain range on a structure's forced harmonic response can be treated as a series of variations in nonlinear parameters and/or excitation levels. As depicted in Fig. 1, if the interested range of the excitation frequency $\omega$ is on the interval $[\omega_l, \omega_h]$, the modifications of the forced harmonic response can be easily obtained.

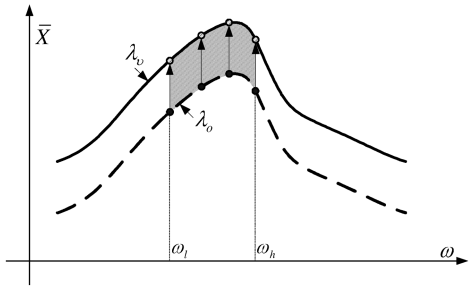


**Fig. 1 An illustration of the solution procedure of the present method.**

## IV. Application

In this section, three numerical examples are included to demonstrate the application and implementation of the proposed method. First, a cantilever beam with a nonlinear element is studied to validate the effectiveness of the proposed method in computing the nonlinear response in the frequency domain. Second, a spring-mass system with local nonlinearities is used to show the present method's application in calculating the steady-state response of a local nonlinear structure when its nonlinear parameter is modified. The results are compared with those obtained by Newmark's method to validate the present approach. Finally, a large-order FE model of a satellite with some nonlinear connectors is used to show the application of the proposed method for studying the relationship among the dynamic response of the satellite's payloads and excitation level, and the connectors' physical parameters.

### A. Cantilever Beam with a Local Nonlinear Element

Here, the cantilever beam discussed in [29] is used as a numerical example, and it is shown in Fig. 2. The FE model of the beam consists of 10 elements. In this model, each node has a vertical translation DOF and a rotation DOF. Only structural damping is considered in this example. The properties of the beam are listed in Table 1. A sine excitation acts at the translation DOF of the 10th node, and its amplitude is 1 N.

The complex equation of motion in the frequency domain can be given by

$$(H_{1919}\Delta + 1)X_{19} = -H_{1919}F \tag{36}$$

In the example, the $n$ set contains the translational DOF of the 10th node (i.e., $X_{19}$). The $f$ set is identical to the $n$ set, and the $i$ set is empty. Subsequently, the undamped modal data of $X_{19}$ are only extracted. With the modal data, the receptance data $H_{19\,19}$ can be easily obtained. Finally, one can use the proposed method to solve Eq. (36) to find the harmonic response of $X_{19}$. It can be seen that the dimension of nonlinear equations in the proposed method is only two, while the whole number of the beam's DOFs is 20.

First, the nonlinearity of the beam is considered with Coulomb damping ($y = C_d(\dot{x})$) between the translation DOF of the 10th node and the ground. $C_d$ is set to be 0.45 N. Then, the fundamental harmonic response of $X_{19}$ around the first linear resonance is shown in Fig. 3a. Second, the nonlinearity is replaced with the cubic stiffness nonlinearity ($y = \beta x^3$). The cubic stiffness coefficient $\beta$ is set to be $1.0 \times 10^8$ N m$^{-3}$. The fundamental harmonic response of $X_{19}$ for this case is shown in Fig. 3b. In both figures, the linear harmonic response is also plotted for comparison. Subsequently, the results obtained by the method presented in [29] are also potted in the figures to validate the accuracy of the results. It can be found that both results are nearly identical. Note that, in Fig. 3b, the response between B and C obtained by the present method is unstable and cannot be realized by the method in [29] or any experiment.

### B. Eight-Degree-of-Freedom Spring-Mass System with a Local Modification

Figure 4 shows an 8-DOF spring-mass system. The parameters used in the example are $m_1 = m_2 = \cdots = m_8 = 1$ kg, and $k_1 = k_2 = \cdots = k_8 = 300$ N m$^{-1}$. A local nonlinear element is added between $m_6$ and $m_7$. It is considered as a spring with cubic stiffness nonlinearity. The mass $m_2$ is subjected to a sine force excitation of amplitude 100 N. The excitation frequency is 2.69 Hz.

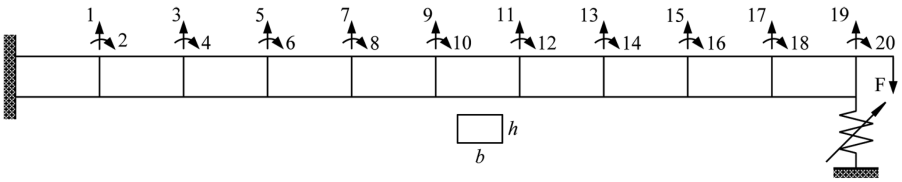


**Fig. 2 A cantilever beam with a nonlinear element.**

**Table 1 Properties of the cantilever beam**

| Parameters | Values |
|---|---|
| Length, $L$ | 0.787 m |
| Width, $b$ | 0.0635 m |
| Height, $h$ | 0.0127 m |
| Modulus of elasticity, $E$ | $2.0 \times 10^{11}$ N m$^{-2}$ |
| Density, $\rho$ | $7.8 \times 10^{3}$ kg m$^{-3}$ |
| Coefficient of structural damping, $G$ | 0.02 |

In the calculations of the example, the damping of the system is assumed to be

$$\mathbf{C} = 2\xi(\boldsymbol{\phi}^T)^{-1}\mathrm{diag}(\omega_1, \ \ldots, \ \omega_8)\boldsymbol{\phi}^{-1}$$

where $\xi$ is set to be 0.015.

The complex equations of motion of the spring-mass system in the frequency domain are

$$\left(\frac{3}{4}\beta\|X_6 - X_7\|^2\begin{bmatrix} H_{66} & H_{67} \\ H_{76} & H_{77}\end{bmatrix}\begin{bmatrix} 1 & -1 \\ -1 & 1\end{bmatrix} + \begin{bmatrix} 1 & 0 \\ 0 & 1\end{bmatrix}\right)\begin{Bmatrix} X_6 \\ X_7\end{Bmatrix} = \begin{pmatrix} H_{62} \\ H_{72}\end{pmatrix}F \tag{37}$$

$$\frac{3}{4}\beta\|X_6 - X_7\|^2[\,H_{86} \quad H_{87}\,]\begin{bmatrix} 1 & -1 \\ -1 & 1\end{bmatrix}\begin{Bmatrix} X_6 \\ X_7\end{Bmatrix} + X_8 = H_{82}F \tag{38}$$

In the current case, the $n$ set includes the translation DOFs of $m_6$ and $m_7$. The $f$ set and the $i$ set contain the translation DOFs of $m_2$ and $m_8$, respectively. Subsequently, the modal data associated with the DOFs in these sets are extracted. With the modal data, the receptance data $H_{66}$, $H_{67}$, $H_{77}$, $H_{62}$, $H_{72}$, $H_{82}$, $H_{86}$, and $H_{87}$ in Eqs. (37) and (38) can be easily calculated.

First, the coefficient $\beta$ of the cubic stiffness nonlinearity is set to be $2.0 \times 10^5$ N m$^{-3}$. The initial solutions of the responses of $m_6$ and $m_7$ are set to be their linear response. The scalar parameter of the pseudoarclength continuation scheme is chosen as $\beta$. Then, the steady-state response of $m_8$ can be acquired with the proposed method, as shown in Fig. 5a. When $\beta$ is changed to $2.0 \times 10^8$ N m$^{-3}$, the nonlinear response of $m_6$ and $m_7$ ($\beta = 2.0 \times 10^5$ N m$^{-3}$) can be used as initial solutions. Similarly, the steady-state response of $m_8$ can be obtained and depicted in Fig. 5b. In both cases, the solutions of the Newmark's method are also plotted to validate the results. In Fig. 5a, the results for both methods are nearly identical. However, they are a little different in Fig. 5b. The difference at the peaks of both responses is due to the effects of higher-order harmonics, which are not considered in the current solution.

### C. Satellite with Local Nonlinear Connectors

This example is an application of the proposed method to study the influence of connectors' nonlinearity on the dynamic properties of a new generation geostationary meteorological satellite [30]. An FE model of the satellite, which is modeled in MSC Patran, is depicted in Fig. 6. The whole model is composed of shell elements, beam elements, and lumped mass elements. The number of elements and DOFs of the model are 18,748 and 11,7108, respectively. In the figure, the marker • represents the nonlinear connectors that are taken into account. It is assumed that all of the connectors have the same nonlinear characteristics, and their nonlinearities are dominated in the axial direction, marked with $Z$ in Fig. 6, for the special requirement of the connection design. Springs with cubic stiffness and bilinear macroslip elements are used to model the nonlinear connectors. A fabricated connector and its nonlinear model are sketched in Fig. 7.

The accelerations of nodes connecting to the launch vehicle are usually specified in the analysis of the dynamic response of a satellite. To convert the forced accelerations into harmonic excitations, the large-mass method is applied here. The method is first placing large masses on excitation DOFs and applying external forces on these DOFs. The amplitude of the external forces can be assigned as $m_L A$. The value of the large mass $m_L$ is suggested to be $10^6$ times the whole mass of the satellite.

The complex equations of motion of the satellite in the frequency domain can be described as

$$\mathbf{H}_{nn}\left(\begin{bmatrix} \bar{\mathbf{k}}_1 & & 0 \\ & \ddots & \\ 0 & & \bar{\mathbf{k}}_9\end{bmatrix} + \begin{bmatrix} \bar{\mathbf{c}}_1 & & 0 \\ & \ddots & \\ 0 & & \bar{\mathbf{c}}_9\end{bmatrix}\right)\mathbf{X}_n + \mathbf{X}_n = \mathbf{H}_{nf}\mathbf{P}_f \tag{39}$$

$$\mathbf{H}_{in}\left(\begin{bmatrix} \bar{\mathbf{k}}_1 & & 0 \\ & \ddots & \\ 0 & & \bar{\mathbf{k}}_9\end{bmatrix} + \begin{bmatrix} \bar{\mathbf{c}}_1 & & 0 \\ & \ddots & \\ 0 & & \bar{\mathbf{c}}_9\end{bmatrix}\right)\mathbf{X}_n + \mathbf{X}_i = \mathbf{H}_{if}\mathbf{P}_f \tag{40}$$

where

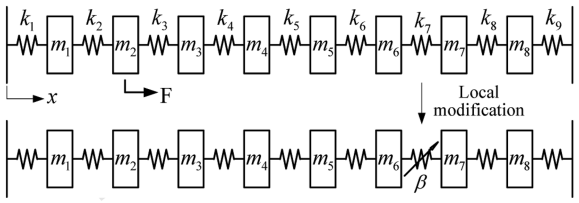


**Fig. 4 An 8-DOF spring-mass system with a local modification.**

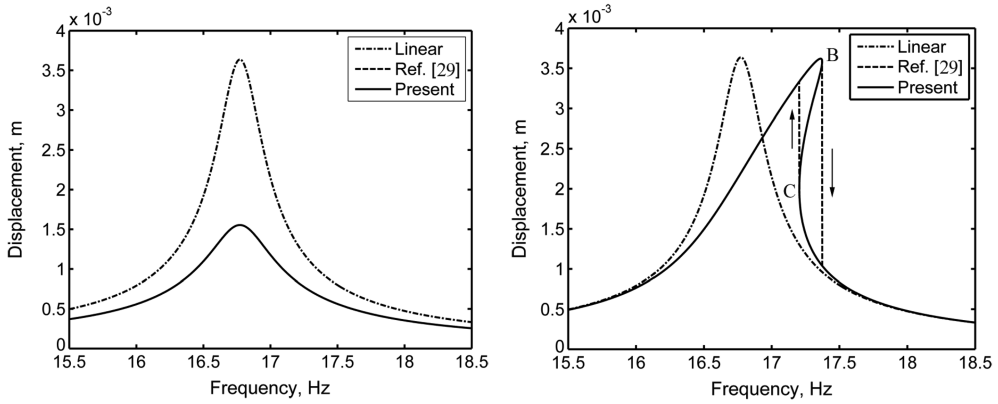


**a) Coulomb damping** **b) Cubic stiffness nonlinearity**

**Fig. 3 Fundamental harmonic response of $X_{19}$ around the first linear resonance frequency.**

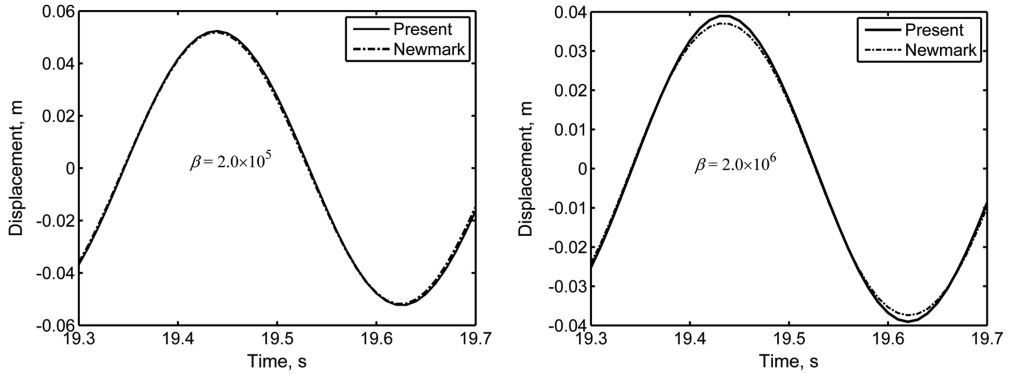


**a) $\beta = 2.0\times10^5$ N m$^{-3}$** **b) $\beta = 2.0\times10^6$ N m$^{-3}$**

**Fig. 5 Comparisons for the response of $m_8$ obtained by the present method and the Newmark's method.**

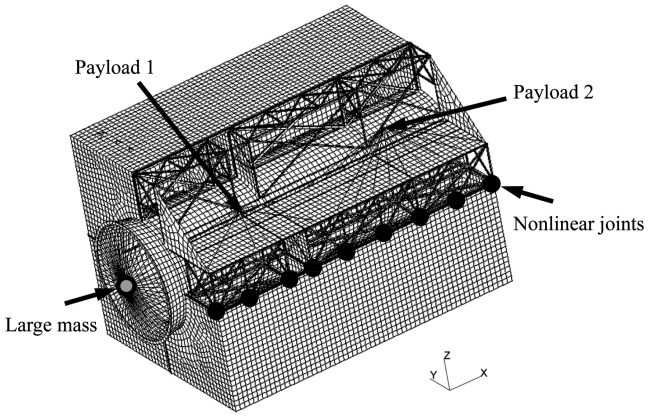


**Fig. 6 An FE model of a satellite with local connectors.**

$$\bar{\mathbf{k}}_r = \frac{3}{4}\beta\|X_{2r-1} - X_{2r}\|^2\begin{bmatrix} 1 & -1 \\ -1 & 1 \end{bmatrix};$$

$$\bar{\mathbf{c}}_r = \begin{bmatrix} \tau_r & -\tau_r \\ -\tau_r & \tau_r \end{bmatrix}; \qquad r = 1, 2, \ldots, 9 \tag{41}$$

and $\tau_r$ is defined as

$$\tau_r = \begin{cases} \frac{z_s}{\pi x_s}\left(\vartheta - \frac{\sin 2\vartheta}{2}\right) + \frac{4jz_s\tilde{x}}{\pi x_s}(1-\tilde{x}) & \|X_{2r-1} - X_{2r}\| \geq x_s \\ z_s/x_s & \|X_{2r-1} - X_{2r}\| < x_s \end{cases} \tag{42}$$

where

$$\tilde{x} = \frac{x_s}{\|X_{2r-1} - X_{2r}\|}$$

and $\vartheta = \arccos(1 - 2\tilde{x})$.

In the launching phase of a satellite, the excitation of the satellite is usually described by defining a vertical acceleration excitation to the nodes of interface connecting to launch vehicle. Since the accelerations of these nodes are generally considered as identical, it is often only one large mass used to connect all nodes by multipoint constraints. Thus, this case can be modeled by assigning an external force in the $x$ direction to the large mass shown in Fig. 6. Meanwhile, the other DOFs of the large mass are constrained. Consequently, in this application, the $n$ set includes all translation DOFs of the nodes in association with the connectors in the $z$ direction; the $i$ set contains the interested DOFs of both payload 1 ($P_1$) and payload 2 ($P_2$); the $f$ set includes the DOF of the large mass in the $x$ direction. Here, 445 modes, which are obtained by MSC Nastran, are used to calculate receptance data when the excitation frequency is in the range of 30 to 100 Hz.

In the study, the number of DOFs that associated with the connectors is only 18. Consequently, with the proposed method, the dimension of nonlinear algebraic equations is 36 (i.e., double the number of nonlinear DOFs). Hence, the computational effort can be greatly reduced.

In the calculation, the structural damping coefficient of the satellite is set to be 0.07, according to the experience of space industries. Numerical calculations are performed to investigate how the physical parameters of nonlinear connectors and the excitation level affect the harmonic response of both payloads. It shows that influences on both payloads are similar. Hence, only the response of $P_2$ is figured and addressed in the following part.

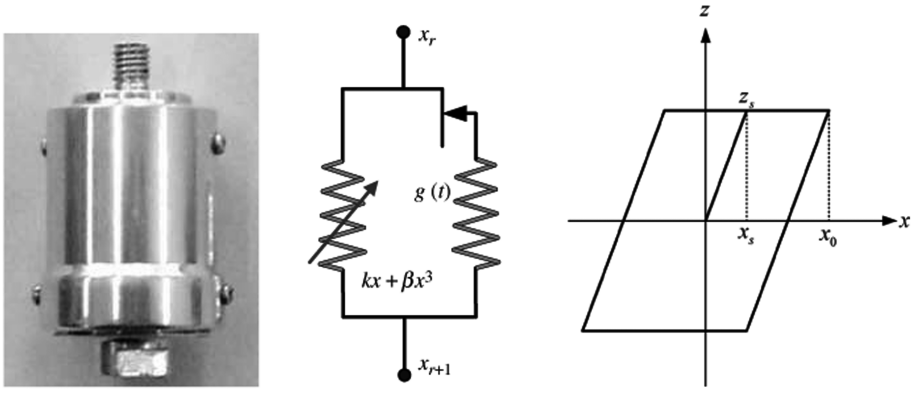


**a)** **b)** **c)**

**Fig. 7 Fabricated connector: a) physical model, b) idealized nonlinear model, and c) characteristic of the bilinear element.**

*1. Effects of $\beta$ ($A = 2$ g, $k = 3.2 \times 10^5$ N m$^{-1}$, $k_s = 4.36 \times 10^7$ N m$^{-1}$, and $z_s = 30$ N)*

The numerical results show that the acceleration harmonic response of $P_2$ around the fourth linear resonance frequency is most obviously affected by the cubic stiffness nonlinearity. Hence, effects of changes in $\beta$ are discussed around the fourth linear resonance frequency, as depicted in Fig. 8. It shows that the amplitude of the resonant vibration increases with the cubic stiffness coefficient $\beta$. The resonant frequency also increases with $\beta$, but the shift of the resonant frequency is small.

*2. Effects of $z_s$ ($k_s = 3.2 \times 10^5$ N m$^{-1}$, $k = 3.2 \times 10^5$ N m$^{-1}$, $A = 2$ g, and $\beta = 7 \times 10^{11}$ N m$^{-3}$)*

Hysteretic damping markedly influences the response when the excitation frequency is in the range of 85 to 100 Hz. Figure 9 shows the acceleration response of $P_2$ versus limiting friction force $z_s$. It can be found that the amplitude of the resonance frequency decreases as the limiting friction force increases.

*3. Effects of $\lambda$ ($\lambda = k_s/k$) ($z_s = 30$ N, $A = 2$ g, and $\beta = 7 \times 10^{11}$ N m$^{-3}$)*

The acceleration of $P_2$ versus the ratio of $k_s$ to $k$ is depicted in Fig. 10. When $\lambda$ is in the range of one to five, the amplitude of the resonant frequency decreases with the increase of $\lambda$. However, when $\lambda$ is larger, it will slightly change.

*4. Effects of Excitation Level A ($k = 3.2 \times 10^5$ N m$^{-1}$, $k_s = 4.36 \times 10^7$ N m$^{-1}$, $z_s = 30$ N, and $\beta = 7 \times 10^{11}$ N m$^{-3}$)*

To show the effects of excitation level $A$, the transmissibility is defined here by $x_r = \ddot{\mathbf{X}}_r/A$. As show in Fig. 11a, the transmissibility of the resonant frequency increases with $A$ when the excitation frequency is in the range of 30 to 44 Hz. It implies that the effects of cubic stiffness nonlinearity increase with $A$. Similarly, as depicted in Fig. 11b, the transmissibility at the resonant frequency also increases along with $A$ when the excitation frequency is in the range of 85 to 105 Hz. However, this means that the effects of hysteretic damping decrease with the increase of $A$.

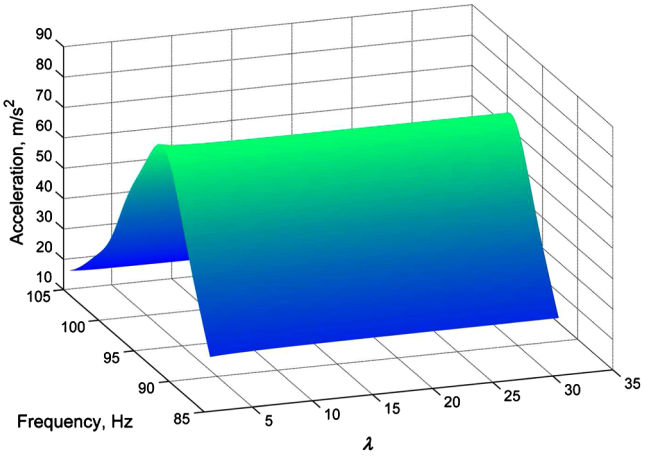


**Fig. 10 Acceleration of $P_2$ versus λ (the ratio of $k_s$ to $k$).**

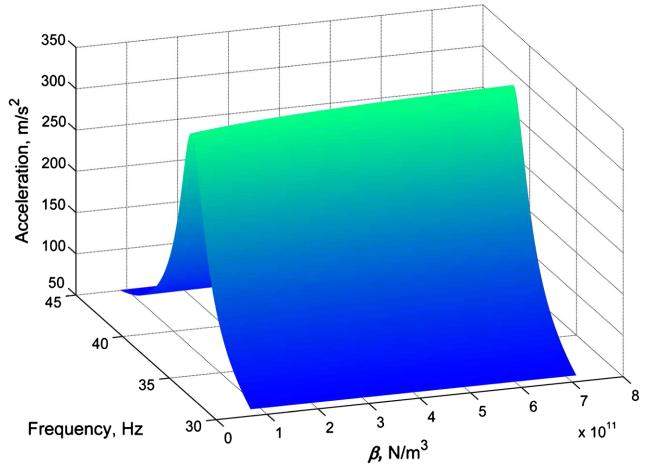


**Fig. 8 Acceleration of $P_2$ versus cubic stiffness coefficient $\beta$.**

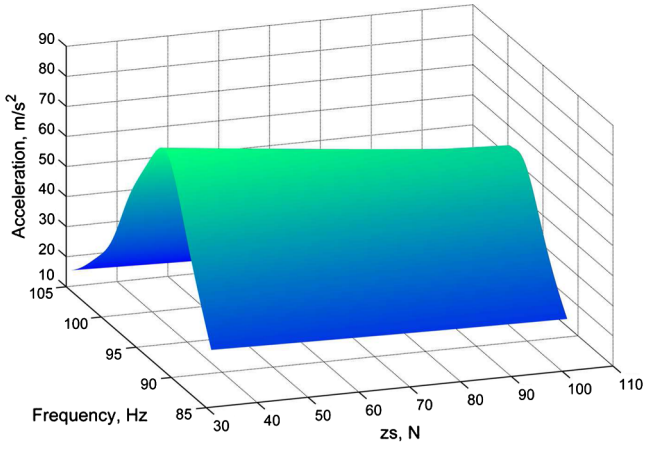


**Fig. 9 Acceleration of $P_2$ versus limiting friction force $z_s$.**

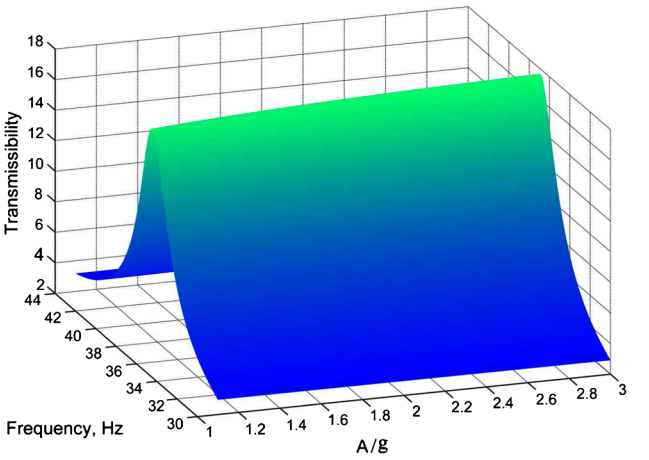


**a) Excitation frequency in the range of 30 to 44 Hz**

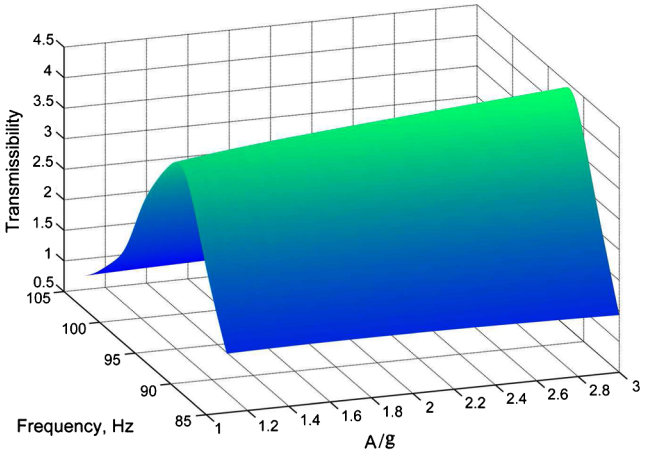


**b) Excitation frequency in the range of 85 to 105 Hz**

**Fig. 11 Transmissibility of $P_2$ versus excitation level $A$.**

## V. Conclusions

In this paper, a method combining the DF with the pseudoarclength continuation scheme and linear receptance is presented for investigating the effects of changes in nonlinear parameters and/or excitation levels on the dynamics of structures with local nonlinearities. With linear receptance data, the computational effort is greatly reduced; thus, the method is applicable to large-scale and complicated structures The proposed method can also be applied to study the steady-state periodic response of nonlinear structures. The proposed method is validated by two numerical examples. In addition, with an application to study the nonlinear connectors of a satellite with payloads, the numerical results show that the nonlinearity of the connector can have a considerable influence on the dynamics of the satellite's payloads.

In the study, only fundamental harmonic is considered. If the nonlinearities of structures are weak or symmetrical, the current method is usually sufficient. Otherwise, high-order harmonics should be involved in order to improve the accuracy. It should be noted that the limitation of the present method is that the dynamic response of the structures is assumed to be periodic.

## References


[1] Ferri, A. A., "Modeling and Analysis of Sleeve Joints of Large Space Structures," *Journal of Spacecraft and Rockets*, Vol. 25, No. 5, 1988, pp. 354–360. doi:10.2514/3.26012

[2] Borden, M., and Dugundji, J., "Joint Damping and Nonlinearity in Dynamics of Space Structures," *AIAA Journal*, Vol. 28, No. 4, 1990, pp. 740–749. doi:10.2514/3.10454

[3] Shi, G., and Atluri, S. N., "Nonlinear Dynamic Response of Frame-Type Structures with Hysteretic Damping at the Joints," *AIAA Journal*, Vol. 30, No. 1, 1992, pp. 234–240. doi:10.2514/3.10904

[4] Bindemann, C., and Ferri, A. A., "Large Amplitude Vibration of a Beam Restrained By a Non-Linear Sleeve Joint," *Journal of Sound and Vibration*, Vol. 184, No. 1, 1995, pp. 19–34. doi:10.1006/jsvi.1995.0302

[5] Yoshida, T., "Dynamic Characteristic Formulations for Jointed Space Structures," *Journal of Spacecraft and Rockets*, Vol. 43, No. 4, 2006, pp. 771–779. doi:10.2514/1.15537

[6] Nayfeh, A. H., and Mook, D. T., *Nonlinear Oscillation*, Wiley, New York, 1979.

[7] Gelb, A., and van der Velde, W. E., *Multiple-Input Describing Functions and Nonlinear System Design*, McGraw–Hill, New York, 1968.

[8] Cameron, T. M., and Griffin, J. H., "An Alternating Frequency/Time Domain Method for Calculating the Steady-State Response of Nonlinear Dynamic Systems," *Journal of Applied Mechanics*, Vol. 56, No. 1, 1989, pp. 149–154. doi:10.1115/1.3176036

[9] Tanrikulu, Ö., Kuran, B., and Özgüven, H. N., İmregün, M., "Forced Harmonic Response Analysis of Nonlinear Structures Using Describing Functions," *AIAA Journal*, Vol. 31, No. 7, 1993, pp. 1313–1320. doi:10.2514/3.11769

[10] Ciğerogğlu, E., and Özgüven, H. N., "Nonlinear Vibration Analysis of Bladed Disks with Dry Friction Dampers," *Journal of Sound and Vibration*, Vol. 295, Nos. 3–5, 2006, pp. 1028–1043. doi:10.1016/j.jsv.2006.02.009

[11] Ferreira, J. V., and Serpa, A. L., "Application of the Arc-length Method in Nonlinear Frequency Response," *Journal of Sound and Vibration*, Vol. 284, Nos. 1–2, 2005, pp. 133–149. doi:10.1016/j.jsv.2004.06.025

[12] Crisfield, M. A., *Non-Linear Finite Element Analysis of Solids and Structures*, Vol. 1, John Wiley, New York, 1997, Chap. 9.

[13] Friswell, M. I., Penny, J. E. T., and Garvey, S. D., "Using Linear Model Reduction to Investigate the Dynamics of Structures with Local Nonlinearities," *Mechanical Systems and Signal Processing*, Vol. 9, No. 3, 1995, pp. 317–328. doi:10.1006/mssp.1995.0026

[14] Shiau, T. N., and Jean, A. N., "Prediction of Periodic Responses of Flexible Mechanical Systems with Nonlinear Characteristics," *Journal of Vibration and Acoustics*, Vol. 112, No. 4, 1990, pp. 501–507. doi:10.1115/1.2930135

[15] Fey, R. H. B., van Campen, D. H., and de Kraker, A., "Long Term Structural Dynamics of Mechanical Systems with Local Nonlinearities," *Journal of Vibration and Acoustics*, Vol. 118, No. 2, 1996, pp. 147–153. doi:10.1115/1.2889642

[16] Moon, B. Y., and Kang, B. S., "Vibration Analysis of Harmonically Excited Non-Linear System Using the Method of Multiple Scales," *Journal of Sound and Vibration*, Vol. 263, No. 1, 2003, pp. 1–20. doi:10.1016/S0022-460X(02)01016-7

[17] Qu, Z. Q., "Model Reduction for Dynamical Systems with Local Nonlinearities," *AIAA Journal*, Vol. 40, No. 2, 2002, pp. 327–333. doi:10.2514/2.1649

[18] Wei, F., and Zheng, G. T., "Nonlinear Vibration Analysis of Spacecraft with Local Nonlinearity," *Mechanical Systems and Signal Processing*, Vol. 24, No. 2, 2010, pp. 481–490. doi:10.1016/j.ymssp.2009.07.005

[19] Sundararajan, P., and Noah, S. T., "Dynamics of Forced Nonlinear Systems Using Shooting Arc-Length Continuation Method-Application to Rotor Systems," *Journal of Vibration and Acoustics*, Vol. 119, No. 1, 1997, pp. 9–20. doi:10.1115/1.2889694

[20] Sundararajan, P., and Noah, S. T., "An Algorithm for Response and Stability of Large Order Nonlinear Systems-Application to Rotor Systems," *Journal of Sound and Vibration*, Vol. 214, No. 4, 1998, pp. 695–723. doi:10.1006/jsvi.1998.1614

[21] Padmanabhan, C., and Singh, R., "Analysis of Periodically Excited Nonlinear Systems by a Parametric Continuation Technique," *Journal of Sound and Vibration*, Vol. 184, No. 1, 1995, pp. 35–58. doi:10.1006/jsvi.1995.0303

[22] von Groll, G., and Ewins, D. J., "The Harmonic Balance Method with Arc-Length Continuation in Rotor Stator Contact Problems," *Journal of Sound and Vibration*, Vol. 241, No. 2, 2001, pp. 223–233. doi:10.1006/jsvi.2000.3298

[23] Kim, T. C., Rook, T. E., and Singh, R., "Effect of Nonlinear Impact Damping on the Frequency Response of a Torsional System with Clearance," *Journal of Sound and Vibration*, Vol. 281, Nos. 3–5, 2005, pp. 995–1021. doi:10.1016/j.jsv.2004.02.038

[24] Ribeiro, P., "Nonlinear Vibrations of Simply-Supported Plates by the *P*-Version Finite Element Method," *Finite Elements in Analysis and Design*, Vol. 41, Nos. 9–10, 2005, pp. 911–924. doi:10.1016/j.finel.2004.12.002

[25] Ribeiro, P., "Non-Linear Free Periodic Vibrations of Open Cylindrical Shallow Shells," *Journal of Sound and Vibration*, Vol. 313, Nos. 1–2, 2008, pp. 224–245. doi:10.1016/j.jsv.2007.11.029

[26] Allgower, E. L., and Georg, K., *Numerical Continuation Methods: An Introduction*, Springer–Verlag, New York, 1990. Chaps. 3, 6.

[27] Allgower, E. L., and Georg, K., "Continuation and Path Following," *Acta Numerica*, Vol. 2, 1993, pp. 1–64. doi:10.1017/S0962492900002336

[28] Keller, H. B., *Lecture Notes on Numerical Methods in Bifurcation Problems*, Springer–Verlag, New York, 1987.

[29] Kuran, B., and Özgüven, H. N., "A Modal Superposition Method for Nonlinear Structures," *Journal of Sound and Vibration*, Vol. 189, No. 3, 1996, pp. 315–339. doi:10.1006/jsvi.1996.0022

[30] Zhang, J., Liang, L., Liu, M. H., Bai, S. J., and Zheng, G. T., "Floating Design of Meteorological Satellite Structure for Thermal Stress Release and Vibration Attenuation," AIAA Space 2008 Conference and Exposition, AIAA Paper 2008-7625, 2008.


F. Pai
*Associate Editor*